

Since Alice only knows the statistical CSI of wireless-related links, the average detection error probability with statistical CSI is adopted as the covertness performance of the system.

Theorem 1. The average detection error probability at Willie with optimal detection threshold can be derived as

$$\bar{\xi}(\tau^*) = 1 - \frac{1}{\Gamma(N_w)} \int_0^{\infty} \gamma \left(n, n \left(\frac{\sigma_w^2}{\sigma_a^2} + 1 \right) \ln \left(1 + \frac{x P_a}{\sigma_w^2} \right) \right) \frac{1}{x} dx. \quad (4)$$

Since Alice only knows the statistical CSI of wireless-related links, the average detection error probability with statistical CSI is adopted as the covertness performance of the system. where B is the parameter of Gaussian-Chebyshev Quadrature, $\theta_b = \frac{\pi}{4} \left(1 + \cos \left(\frac{(2b-1)\pi}{2B} \right) \right)$, and $f(x) = \frac{e^{-\frac{x}{\lambda_w}} x^{N_w-1}}{\lambda_w^{N_w} \Gamma(N_w)}$. The average detection error probability at Willie with optimal detection threshold can be derived as

Proof. We denote $X_k = \mathbf{h}_{rw,k}^H \mathbf{\Theta} \mathbf{h}_{ar}$, which approximately follows the complex Gaussian distribution, i.e., $X_k \sim \mathcal{CN}(0, N_r \frac{n P_a}{r_w \lambda_w})$, when N_r is sufficiently large [?]. The tightness of this approximation is validated by [?] and Section VI over N_r is relatively small. Thus, $f(\tan \theta_b)$ follows the Gamma Distribution with the probability density function (PDF) $f(x) = \frac{e^{-\frac{x}{\lambda_w}} x^{N_w-1}}{\lambda_w^{N_w} \Gamma(N_w)}$ [?]. By substituting (??) into (??), where B is the parameter of Gaussian-Chebyshev Quadrature, the average detection error probability can be expressed as

$$\bar{\xi}(\tau^*) = 1 - \frac{1}{\Gamma(N_w)} \int_0^{\infty} \gamma \left(n, n \left(\frac{\sigma_w^2}{\sigma_a^2} + 1 \right) \ln \left(1 + \frac{x P_a}{\sigma_w^2} \right) \right) \frac{1}{x} dx. \quad (5)$$

Proof. We denote $X_k = \mathbf{h}_{rw,k}^H \mathbf{\Theta} \mathbf{h}_{ar}$, which approximately follows the complex Gaussian distribution, i.e., $X_k \sim \mathcal{CN}(0, N_r \frac{n P_a}{r_w \lambda_w})$, when N_r is sufficiently large [?]. The tightness of this approximation is validated by [?] and Section VI even N_r is relatively small. Thus, $f(\tan \theta_b)$ follows the Gamma distribution with the probability density function (PDF) $f(x) = \frac{e^{-\frac{x}{\lambda_w}} x^{N_w-1}}{\lambda_w^{N_w} \Gamma(N_w)}$ [?]. By substituting (??) into (??), the average detection error probability can be expressed as

Due to the complicated form of (??), it is intractable to guide the system design. To address this issue, we derive a tractable approximation of the detection error probability as follows.

Lemma 1. In high covertness scenarios with moderate blocklength (such as $n \geq 50$), the average detection error probability at Willie can be approximated as

$$\bar{\xi}(\tau^*) \approx 1 - \sqrt{\frac{n P_a \lambda_w}{2\pi \sigma_w^2}}. \quad (7)$$

By substituting $x = \tan \theta$ into (??) and applying Gaussian-Chebyshev Quadrature, the average detection error probability can be obtained, and the proof is completed. \square

$$\bar{\xi}(\tau^*) \approx 1 - \sqrt{\frac{n P_a \lambda_w}{2\pi \sigma_w^2}}. \quad (8)$$

Due to the complicated form of (??), it is intractable to guide system design. To address this issue, we derive a tractable approximation of the detection error probability as follows.

Thus, the average detection error probability is derived as Lemma 1. In high covertness scenarios with moderate blocklength (such as $n \geq 50$), the average detection error probability at Willie can be approximated as

$$\bar{\xi}(\tau^*) \approx 1 - \sqrt{\frac{n P_a \lambda_w}{2\pi \sigma_w^2}}. \quad (9)$$

Proof. The detection error probability (??) is approximated as $\frac{1}{\Gamma(N_w)} \int_0^{\infty} \gamma \left(N_w, \frac{\sigma_w^2}{\lambda_w P_a} \ln \left(\frac{2\pi}{\sigma_w^2} \right) \right) \frac{1}{x} dx$, which can be ignored compared with other terms due to $\lim_{P_a \rightarrow 0} \frac{1}{P_a} \ln \left(\frac{2\pi}{\sigma_w^2} \right) = 0$. \square

The concise expression (??) implies that the $\bar{\xi}(\tau^*)$ is linear to \sqrt{n} , N_w , and P_a in high covertness scenarios, facilitating the performance analysis in Section V. Besides, the tightness of (??) is also validated in Section VI.

Thus, the average detection error probability is derived as When Alice transmits, the received signal at Bob is

$$y_b[i] = (h_{ab} + \mathbf{h}_{rb}^H \mathbf{\Theta} \mathbf{h}_{ar}) x[i] + n_b[i]. \quad (10)$$

Based on the received signal (??), Bob can decode the messages. However, the decoding error can not be ignored due to finite blocklength, which is given by [?]

$$g_b(P_a) = \mathbb{Q} \left(\sqrt{\frac{2\pi}{n}} \sqrt{\frac{P_a}{\sigma_b^2}} \left(1 + \frac{N_b}{N_r} + 1 \right) \right) \sqrt{\frac{2\pi}{n}} \quad (11)$$

where $g_b(P_a)$ denotes the received SNR at Bob, and R is the transmission rate measured by bits per channel use (bpcu). Since the decoding error probability is affected by fading channels, the average decoding error probability is adopted to evaluate the reliability performance.

IRS can adjust its reflection coefficients at each transmission round to maximize γ_b , where the optimal phase is given by $\theta_i^* = \arg(h_{ab}) + \arg(h_{rb,i}) - \arg(h_{ar,i})$, $h_{ar,i}$ and $h_{rb,i}$ denote the channel from Alice to the i -th element at Bob IRS, and from the i -th element to Bob, respectively. Thus, the instantaneous SNR can be expressed as $\gamma_b = X^2 P_a / \sigma_b^2$ where

$$X = |h_{ab}| + \sum_{i=1}^N |h_{rb,i}| |h_{ar,i}|. \quad (12)$$

Based on the received signal (??), Bob can decode the messages. However, the decoding error can not be ignored due to finite blocklength, which is given by [?]

X can be approximated by a generalized Gamma distribution with PDF $f_X(x) = \frac{\beta^\alpha}{\Gamma(\alpha)} x^{\alpha-1} e^{-\beta x} / \Gamma(\alpha)$, where $\alpha = \Psi^2 / \Phi$, $\beta = \Psi / \Phi$, $\Psi = \alpha_d \beta_d + N_r \alpha_r / \beta_r$, $\Phi = \alpha_d / \beta_d + N_r \alpha_r / \beta_r$, $\alpha_d = \frac{\pi}{4-\pi}$, $\beta_d = \frac{2\sqrt{\pi}}{(4-\pi)\sqrt{\lambda_{ab}}}$, $(\alpha_r + \beta_r)^{-2} \frac{\pi^2}{16-\pi^2}$ and $\beta_r = \frac{4\pi}{(16-\pi^2)\sqrt{\lambda_{ab}}}$. Then, the PDF of γ_b is derived as

where $\gamma_b = |h_{ab} + \mathbf{h}_{rb}^H \mathbf{\Theta} \mathbf{h}_{ar}|^2 P_a / \sigma_b^2$ denotes the received SNR at Bob, and R is the transmission rate measured by bits per channel use (bpcu). Since the decoding error probability (??) is affected by fading channels, the average decoding error probability can be derived as

IRS can adjust its reflection coefficients at each transmission round to maximize γ_b , where the optimal phase is given by $\theta_i^* = \arg(h_{ab}) + \arg(h_{rb,i}) - \arg(h_{ar,i})$, $h_{ar,i}$ and $h_{rb,i}$ denote the channel from Alice to the i -th element at IRS, and from the i -th element to Bob, respectively. Thus, the instantaneous SNR can be expressed as $\gamma_b = X^2 P_a / \sigma_b^2$ where

$$X = |h_{ab}| + \sum_{i=1}^N |h_{rb,i}| |h_{ar,i}|. \quad (13)$$

where step (a) is due to linear approximation of Q -function [?], X can be approximated by a generalized Gamma distribution with PDF $f_X(x) = \frac{\beta^\alpha}{\Gamma(\alpha)} x^{\alpha-1} e^{-\beta x} / \Gamma(\alpha)$, where $\alpha = \Psi^2 / \Phi$, $\beta = \Psi / \Phi$, $\Psi = \alpha_d \beta_d + N_r \alpha_r / \beta_r$, $\Phi = \alpha_d / \beta_d + N_r \alpha_r / \beta_r$, $\alpha_d = \frac{\pi}{4-\pi}$, $\beta_d = \frac{2\sqrt{\pi}}{(4-\pi)\sqrt{\lambda_{ab}}}$, $(\alpha_r + \beta_r)^{-2} \frac{\pi^2}{16-\pi^2}$ and $\beta_r = \frac{4\pi}{(16-\pi^2)\sqrt{\lambda_{ab}}}$.

and V_r . The theoretical predictions about required reflection elements as

In this section, the reliability performance is derived under the covertness requirement $\xi(\tau^*) \geq \frac{1}{2} - \epsilon$, where ϵ is a predetermined value to evaluate the covertness level. Besides, we provide the theoretical predictions about the number of reflection elements required to achieve a decoding error probability close to 0 with given covertness requirements.

On the one hand, $\xi(\tau^*)$ decreases with N_r as shown in (??), which implies that the allowed transmit power P_a also decreases with N_r to meet the covertness requirement $\xi(\tau^*) \geq 1 - \epsilon$. On the other hand, $\xi(\tau^*)$ decreases with N_r and P_a as shown in (??). Therefore, the reliability guarantee by IRS is unclear but crucial, and the question that how many reflection elements are required to achieve a decoding error probability close to 0 with covertness requirements is significant.

To address this issue, we first derive the reliability performance in high covertness scenarios when $N_r \rightarrow \infty$ as follows:

Theorem 2. When $N_r \rightarrow \infty$, the achievable average decoding error probability with given ϵ in high covertness scenarios is

$$\lim_{N_r \rightarrow \infty} \bar{\delta} = \begin{cases} \frac{(2\alpha\nu+1)}{2} - \sqrt{\frac{2\alpha\nu}{16\sigma^2\lambda_{r,w}}}, & r_1 \leq r_{rw} < r_2 \\ 0, & r_2 \leq r_{rw} \end{cases} \quad (14)$$

In this section, the reliability performance is derived under the covertness requirement $\xi(\tau^*) \geq \frac{1}{2} - \epsilon$, where ϵ is a predetermined value to evaluate the covertness level. where $r_{rw} = \lim_{N_r \rightarrow \infty} \frac{N_r}{N_w}$ denotes the ratio of the number of reflection elements at IRS to that of antennas at Willie. $r_1 = \frac{1}{\sqrt{16\lambda_{r,w}\sigma_b^2}}$ and $r_2 = \frac{1}{\sqrt{16\lambda_{r,w}\sigma_a^2}}$ are the critical factors in high covertness scenarios. Proof: See Appendix ??.

On the one hand, $\xi(\tau^*)$ decreases with N_r as shown in (??), which gives the theoretical predictions about the number of reflection elements required to achieve high-reliability performance. On the other hand, $\bar{\delta}$ decreases with N_r when $N_r \rightarrow \infty$ as shown in (14). Specifically, when $N_r \rightarrow \infty$, the decoding error probability approaches 0. Besides, when $N_r < r_1 N_w$, the decoding error probability approaches 1. Moreover, it shows that the covertness requirements ϵ , the blocklength n , and the transmission rate R all affect the critical factors in high covertness scenarios. Specifically, the tighter the covert requirement, the longer the blocklength and the higher the transmission rate, the more reflection elements are required to guarantee high-reliability performance.

Theorem 2. When $N_r \rightarrow \infty$, the achievable average decoding error probability with given ϵ in high covertness scenarios is

When the number of reflection elements at IRS (antennas at Willie) is finite, the decoding error probability can be obtained by substituting the maximum allowed transmit power P_a into (??) by (??) into (??). Finally, we summarize the achievable reliability of IRS-enabled short-packet communication systems under covertness requirements in Table I.

where $r_{rw} = \lim_{N_r \rightarrow \infty} \frac{N_r}{N_w}$ denotes the ratio of the number of reflection elements at IRS to that of antennas at Willie.

In this section, numerical results are provided to evaluate the performance of IRS-enabled short-packet communications. For illustration, we assume that Alice, Bob, Willie, and the

TABLE II
Achievable Decoding Error Probability

Element Number	$N_w, N_r \rightarrow \infty$	$N_w, N_r \rightarrow \infty$	$N_w, N_r \rightarrow \infty$
Element Number	$N_w, N_r \rightarrow \infty$	$r_1 N_w, N_r \rightarrow \infty$	$N_w \leq N_r \rightarrow \infty$
$\bar{\delta}$	$r_{rw} \leq r_1$	$r_1 \leq r_{rw} < r_2$	$r_2 \leq r_{rw}$
Element Number	$N_w \rightarrow \infty$	$N_r \rightarrow \infty$	N_r, N_w
Element Number	N_r finite	N_r finite	N_r finite
$\bar{\delta}$	N_r finite	N_r finite	N_r finite
$\bar{\delta}$	1	0	(??)

Proof. See Appendix ??.

Theorem 2 gives the theoretical predictions about the number of reflection elements required to achieve high-reliability performance ($\bar{\delta} \rightarrow 0$) with $N_w \rightarrow \infty$. Specifically, when $N_r \geq r_2 N_w$, the decoding error probability approaches 0. However, when $N_r < r_1 N_w$, the decoding error probability approaches 1. Besides, when $r_1 N_w \leq N_r < r_2 N_w$, the decoding error probabilities approach values between 0 and 1. Moreover, it shows that the covertness requirements ϵ , the blocklength n and the transmission rate R all affect the critical factors r_1 and r_2 . Specifically, the tighter the covert requirement, the longer the blocklength and the higher the transmission rate, the more reflection elements are required to guarantee high-reliability performance.

When the number of reflection elements at IRS (antennas at Willie) is finite, the decoding error probability can be obtained by substituting the maximum allowed IRS are located at (0,0), (10m,0), (12m,5m), and (10m,1m) in a two-dimensional plane, respectively. The fading parameters are expressed as $\alpha_{ar} = 2.2$, $\alpha_{ab} = 2.2$, $\alpha_{aw} = 3.9$, $\alpha_{bw} = 3.9$. For illustration, we assume that Alice, Bob, Willie, and the IRS are located at (0,0), (10m,0), (12m,5m), and (10m,1m) in a two-dimensional plane, respectively. The fading parameters are expressed as $\alpha_{ar} = 2.2$, $\alpha_{ab} = 2.2$, $\alpha_{aw} = 3.9$, $\alpha_{bw} = 3.9$. For illustration, we assume that Alice, Bob, Willie, and the IRS are located at (0,0), (10m,0), (12m,5m), and (10m,1m) in a two-dimensional plane, respectively. The fading parameters are expressed as $\alpha_{ar} = 2.2$, $\alpha_{ab} = 2.2$, $\alpha_{aw} = 3.9$, $\alpha_{bw} = 3.9$.

In this section, numerical results are provided to evaluate the performance of IRS-enabled short-packet communications. For illustration, we assume that Alice, Bob, Willie, and the IRS are located at (0,0), (10m,0), (12m,5m), and (10m,1m) in a two-dimensional plane, respectively. The fading parameters are expressed as $\alpha_{ar} = 2.2$, $\alpha_{ab} = 2.2$, $\alpha_{aw} = 3.9$, $\alpha_{bw} = 3.9$.

In Figs. 2 (a) and (b), the impacts of the transmit power on the average detection error probability and average decoding error probability are investigated from Fig. 2 (a) and (b). It can be seen that the curves with numerical simulations (the analytical expression (22), and the approximation expression (23) coincide even if the number of reflection elements is relatively small, such as $N_r = 16$. From Fig. 2 (b), it can be seen that the results obtained by (23) are close to those obtained by numerical simulations. If the number of reflection elements is relatively small, such as $N_r = 16$, the detection (decoding) error probabilities decrease with P_a and N_r in Fig. 2 (a) and (b), the impacts of the transmit power on the average detection error probability and average decoding error probability are investigated from Fig. 2 (a) and (b). It can be seen that the curves with numerical simulations (the analytical expression (22), and the approximation expression (23) coincide even if the number of reflection elements is relatively small, such as $N_r = 16$.

In Figs. 2 (a) and (b), the impacts of the transmit power on the average detection error probability and average decoding error probability are investigated from Fig. 2 (a) and (b). It can be seen that the curves with numerical simulations (the analytical expression (22), and the approximation expression (23) coincide even if the number of reflection elements is relatively small, such as $N_r = 16$.

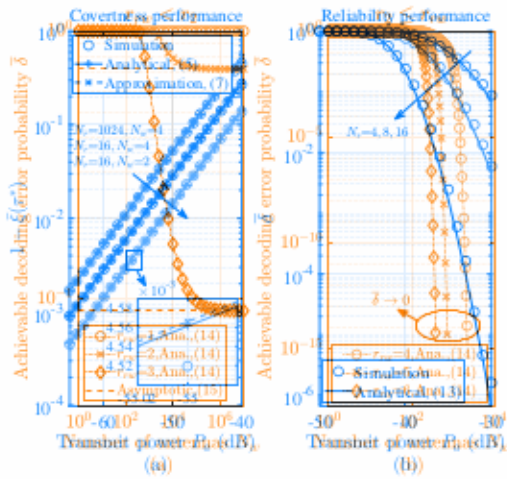


Fig. 2. The achievable decoding error probability versus the decoding error probability versus the transmit power.

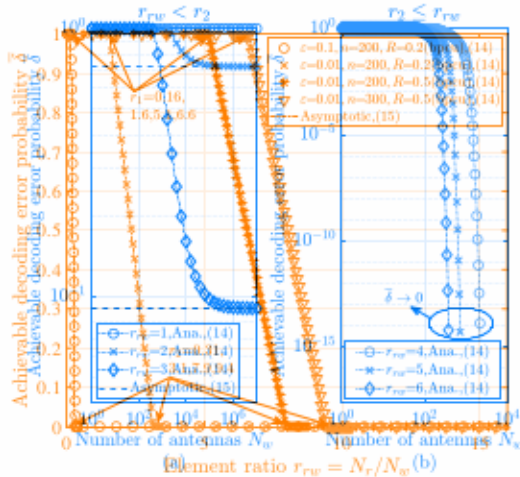


Fig. 3. The achievable decoding error probability versus the number of antennas at Willie.

and reflection elements (b), the decoding error probability are investigated, where the curves with “Ana.” denote the results obtained by (??). It can be seen that the results by (??) tend to the asymptotic ones by (??) as N_w increases. Specifically, from Fig. 5 (a) it can be seen that $\delta \rightarrow 0$ with P_{tx} and $1/N_r$ since more energy is received by Willie (Bob) when IRS is equipped with more reflection elements. These results validate the results given in Sec. 6 in [31], implying that the proposed approximations in (??) and (??) can be used to predict that at least N_r reflection elements at IRS are required for decoding error probabilities to approach 0.

In Fig. 4, the impacts of system parameters on the decoding error probability are investigated, where the number of antennas at Willie is 10^6 and we can see that the curves with (A.22) coincide with the asymptotic ones by (??). Besides, we can observe that the decoding error probability decreases as the covert requirements input system parameters N_w, R, N_r all affect the critical factors. Specifically, when N_w changes from 0.16 (0.34) to 6.6 (9.4), and when ϵ changes

from 0.1 to 0.01. Similarly, r_1 (r_2) changes from 1.6 (3.1) to 5.1 (7.9), when R changes from 0.2 (bpcu) to 0.5 (bpcu). In addition, r_1 (r_2) changes from 0.21 (0.9) to 6.6 (9.4), when n changes from 200 to 300. These results demonstrate that more reflection elements are required to achieve high reliability ($\delta \rightarrow 0$) with tighter covertness requirements, higher transmission rates and longer blocklength, which provides insights for the practical system design.

VII. CONCLUSION

In this paper, we have provided the theoretical prediction about the required number of reflection elements to guarantee covertness and reliability performance in IRS-enabled short-packet communications. To this end, the decoding error probability at Willie has been derived firstly for evaluating the covertness performance, where a concise approximation is also provided to facilitate further analysis. Then, the decoding error probability at Bob has been derived for evaluating the reliability performance. Combined with the above system performance metrics, we have analyzed the required number of reflection elements at IRS to achieve high reliability ($\delta \rightarrow 0$) with covertness requirement $\epsilon(\tau^*) \geq 1 - \epsilon$ in the asymptotic regime. Finally, Monte-Carlo simulations have been provided to evaluate the accuracy of analytical results and the validity of the theoretical predictions. Simulation results have shown that decoding error probabilities approach 0.

In Fig. 4, the impacts of system parameters on the decoding error probability are investigated, where the number of antennas at Willie is 10^6 . It can be seen that the results by (??) coincide with the asymptotic ones by (??).

APPENDIX A PROOF OF THEOREM 2

In high covertness scenarios with $N_r \rightarrow \infty$, the allowed transmit power with given covertness requirement ϵ is $P_a \approx 1.6 \frac{2\pi}{\sqrt{4\pi}} \frac{N_r N_w}{\sqrt{4\pi}} \frac{1}{\sqrt{4\pi}}$. Specifically, r_1 (r_2) changes from 0.16 (0.34) to 1.6 (3.1), when ϵ changes from 0.1 to 0.01. Similarly, r_1 (r_2) changes from 1.6 (3.1) to 5.1 (7.9), when R changes from 0.2 (bpcu) to 0.5 (bpcu). By substituting the allowed transmit power and above approximations into (??), we can obtain from 0.1 (0.34) to 6.6 (9.4), when n changes from 200 to 300. These results demonstrate that more reflection elements are required to achieve high reliability ($\delta \rightarrow 0$) with tighter covertness requirements, higher transmission rates and longer blocklength, which provides insights for the practical system design.

where $f_2(t) = \frac{\gamma \sqrt{\frac{N_r N_w}{\lambda_{r,b} \epsilon \sigma^2}} \sqrt{\frac{N_r N_w \lambda_{r,w} \sigma^2}{\lambda_{r,b} \epsilon \sigma^2}}}{\sqrt{\frac{N_r N_w}{\lambda_{r,b} \epsilon \sigma^2}}}$ and in this paper, we have provided the theoretical prediction about the required number of reflection elements to guarantee covertness and reliability performance in IRS-enabled short-packet communications. To this end, the detection error probability at Willie has been derived firstly, and derive some properties of these functions, first. For the case with $r_1 < 1$ we can obtain that Combined with the above system performance metrics, we have analyzed the required number of reflection elements at IRS to achieve high reliability ($\delta \rightarrow 0$) with covertness requirement $\epsilon(\tau^*) \geq 1 - \epsilon$ in the asymptotic regime.

Finally, step (c) holds since the convexity of $g_2(t) = t^{x-1}e^{-t}$ on $(0, rx]$ with $r < 1, x \rightarrow \infty$, and $\int_0^{rx} g_2(t)dt \leq \frac{rx(g_2(0)+g_2(rx))}{2}$. Step (b) holds due to the asymptotic property of Gamma function as $\lim_{x \rightarrow \infty} \Gamma(x) \leq e^{-x}x^{x-\frac{1}{2}}\sqrt{2\pi}$ by [?, (1.43)]. Step (c) holds due to $\lim_{x \rightarrow \infty} \sqrt{x}e^{x(1-r)}r^x = 0$.

For the case with $r = 1$, we can obtain that

Proof of Theorem 2

In high covertness scenarios with $\frac{\Gamma(x, x)}{\Gamma(x)} \xrightarrow{(a)} \frac{1}{\Gamma(x)}$ as $x \rightarrow \infty$, the allowed transmit power with given covertness requirement ε is where step (a) holds since $\lim_{x \rightarrow \infty} \Gamma(x) = \frac{1}{\Gamma(x)}$ according to the resurgence property of the incomplete Gamma function by [?, (1.2)] and the asymptotic property of Gamma function by [?, (1.43)].

For the case with $r > 1$, we can obtain that

$$1 - \lim_{x \rightarrow \infty, r > 1} f_4(x, r) = \lim_{x \rightarrow \infty, r > 1} \int_{rx}^{\infty} \frac{t^{x-1}e^{-t}}{\Gamma(x)} dt \quad (18)$$

$$\stackrel{(a)}{<} \lim_{x \rightarrow \infty} \frac{(rx)^x e^{-rx}}{\Gamma(x)} \stackrel{(b)}{<} \lim_{x \rightarrow \infty} \frac{\sqrt{rx} e^{x(1-r)}}{\sqrt{2\pi}} \stackrel{(c)}{=} 0, \quad (15)$$

where $f_2(t) = \frac{1}{\Gamma(x)} \int_0^t t^{x-1}e^{-t} dt$ and where the step (a) holds since $g_3(t) = t^{x-1}e^{-t} < g_4(t) = (rx)^{x+1}e^{-rx}t^{-2}$ for $t \geq rx, r > 1, x \rightarrow \infty$, and $\int_{rx}^{\infty} t^{-2}dt = \frac{1}{rx}$. Besides, steps (b) and (c) holds for the same reason as elaborated in the case with $r < 1$. To sum, $\lim_{x \rightarrow \infty} f_4(x, r) = 0$ with $r < 1$, $\lim_{x \rightarrow \infty} f_4(x, r) = \frac{1}{\Gamma(x)}$, and derive some properties of these functions first. For the case with $r < 1$, we can obtain that

By substituting $x = \frac{0}{16-\pi^2}$ and $r = \frac{N_r\pi^2}{16-\pi^2}$ into $f_4(x, r)$ and $f_5(x, r)$, results in Theorem ?? are obtained. where step (a) holds due to the convexity of $g_2(t) = t^{x-1}e^{-t}$ on $(0, rx]$ with $r < 1, x \rightarrow \infty$, and $\int_0^{rx} g_2(t)dt \leq \frac{rx(g_2(0)+g_2(rx))}{2}$. Step (b) holds due to the asymptotic property of Gamma function as $\lim_{x \rightarrow \infty} \Gamma(x) \leq e^{-x}x^{x-\frac{1}{2}}\sqrt{2\pi}$ by [?, (1.43)]. Step (c) holds due to $\lim_{x \rightarrow \infty} \sqrt{x}e^{x(1-r)}r^x = 0$.

For the case with $r = 1$, we can obtain that

$$\lim_{x \rightarrow \infty, r=1} f_4(x, r) = 1 - \lim_{x \rightarrow \infty} \frac{\Gamma(x, x)}{\Gamma(x)} \stackrel{(a)}{=} \frac{1}{\Gamma(x)}, \quad (17)$$

where step (a) holds since $\lim_{x \rightarrow \infty} \Gamma(x, x) = \frac{\gamma(x, rx)}{\Gamma(x)}$ and $f_5(x, r) = \frac{\Gamma(x, rx)}{\Gamma(x)}$, and derive some properties of these functions first. For the case with $r < 1$, we can obtain that

$$1 - \lim_{x \rightarrow \infty, r > 1} f_4(x, r) = \lim_{x \rightarrow \infty, r > 1} \int_{rx}^{\infty} \frac{t^{x-1}e^{-t}}{\Gamma(x)} dt \quad (18)$$

$$\stackrel{(a)}{<} \lim_{x \rightarrow \infty} \frac{(rx)^x e^{-rx}}{\Gamma(x)} \stackrel{(b)}{<} \lim_{x \rightarrow \infty} \frac{\sqrt{rx} e^{x(1-r)}}{\sqrt{2\pi}} \stackrel{(c)}{=} 0,$$

where the step (a) holds since $g_3(t) = t^{x-1}e^{-t} < g_4(t) = (rx)^{x+1}e^{-rx}t^{-2}$ for $t \geq rx, r > 1, x \rightarrow \infty$, and $\int_{rx}^{\infty} t^{-2}dt = \frac{1}{rx}$. Besides, steps (b) and (c) holds for the same reason as elaborated in the case with $r < 1$.

To sum, $\lim_{x \rightarrow \infty} f_4(x, r) = 0$ with $r < 1$, $\lim_{x \rightarrow \infty} f_4(x, r) = \frac{1}{\Gamma(x)}$ with $r = 1$, and $\lim_{x \rightarrow \infty} f_4(x, r) = 1$ with $r > 1$. Similarly, we can obtain $\lim_{x \rightarrow \infty} f_5(x, r) = 0$ with $r > 1$, $\lim_{x \rightarrow \infty} f_5(x, r) = \frac{1}{\Gamma(x)}$ with $r = 1$, and $\lim_{x \rightarrow \infty} f_5(x, r) = 1$ with $r < 1$.

By substituting $x = \frac{N_r\pi^2}{16-\pi^2}$ and $r = \frac{4}{\pi} \sqrt{\frac{N_w\lambda_{rw}\sigma_w^2}{N_r\lambda_{rb}\varepsilon\sigma_w^2}} \sqrt{\frac{\pi}{2\pi}} \left(\omega + \frac{1}{2\nu}\right)$ into $f_4(x, r)$ and $f_5(x, r)$, results in Theorem ?? are obtained.